Applied Catalysis B: Environmental 90 (2009) 83–88

Contents lists available at ScienceDirect

Applied Catalysis B: Environmental

journal homepage: www.elsevier.com/locate/apcatb

Evaluation of catalysts for N_2O abatement in fluidized-bed combustion

Marta Santiago [a], Miguel A.G. Hevia [a], Javier Pérez-Ramírez [a,b,*]

[a] Laboratory for Heterogeneous Catalysis, Institute of Chemical Research of Catalonia (ICIQ), Avinguda Països Catalans 16, 43007, Tarragona, Spain
[b] Catalan Institution for Research and Advanced Studies (ICREA), Passeig Lluís Companys 23, 08010, Barcelona, Spain

ARTICLE INFO

Article history:
Received 3 January 2009
Received in revised form 18 February 2009
Accepted 19 February 2009
Available online 28 February 2009

Keywords:
N_2O abatement
Fluidized-bed combustion
Iron zeolite
Spinel
Perovskite
Hexaaluminate
Sulfur tolerance

ABSTRACT

Several catalysts, including FeZSM-5, Co_2AlO_4, $LaCoO_3$, and $BaFeAl_{11}O_{19}$, were evaluated for N_2O decomposition under representative flue-gas conditions in fluidized-bed combustion (FBC). Closely related formulations proved active and stable catalysts for process-gas or tail-gas de-N_2O in nitric acid plants. With this as starting point, their potential suitability for N_2O abatement in stationary combustion was assessed. Tests were carried out in a fixed-bed reactor at ambient pressure and in the temperature range of 473–1123 K using mixtures of N_2O, O_2, NO, CO, SO_2, and H_2O. The mixed oxide catalysts were strongly inhibited by water and sulfur dioxide and experienced fast deactivation in the simulated mixture containing all the gases. Bulk sulfate phases were detected by X-ray diffraction in the used perovskite and hexaaluminate, revealing insufficient chemical stability in the presence of sulfur and discouraging installation in the freeboard of the combustor. In great contrast, the activity of steam-activated FeZSM-5 in the model and simulated mixtures was comparable, rendering very stable performance during 30 h on stream. The unique tolerance of this iron zeolite to the complex combination of feed components makes it prone to implementation after the cyclone of FBCs, where temperatures are typically 800–1100 K.

1. Introduction

The energy demand grows exponentially due to the increasing consumption in developed countries and the electrification of the Third World. Among fossil fuels, coal is the most vital energy resource, providing more than 40% of the World electric power. The coal consumption pace will probably remain and even increase due to its higher abundance and more even distribution around the globe compared to oil and gas [1].

The concern associated with SO_x and NO_x emissions from coal-fired power plants led to the necessity of developing environmentally friendlier combustion technology, such as fluidized-bed combustion (FBC). Fluidized-bed combustors operate at a relatively low combustion temperature (1023–1173 K), leading to lower emission levels of NO_x and optimal conditions for sulfur capture by limestone or dolomite [2]. They are also versatile with respect to the type of fuel (fossil, biomass, and general waste). Unfortunately, these merits are off-set by a strongly increased emission of N_2O, reaching values up to 600 ppm depending on the combustion temperature, type of combustor, and fuel used [3–5]. The most important pathways that lead to N_2O are the homogeneous oxidation of N-groups in volatiles (mainly HCN) and heterogeneous reactions (direct oxidation of char-N and the reaction of char-N with NO) [4].

Anthropogenic N_2O emissions have become increasingly under review by environmental authorities over the last decade due to its recognized action as a powerful greenhouse gas and its inclusion in the Kyoto protocol. A number of catalysts based on bulk and supported mixed metal oxides and metal-loaded zeolites have been implemented for N_2O decomposition in adipic acid plants (e.g. $CuAl_2O_4/Al_2O_3$ and Ag/Al_2O_3 by BASF, $CoO–NiO/ZrO_2$ by DuPont, and CuO/Al_2O_3 by Asahi Chemical) [6] and in nitric acid plants (CuO/Al_2O_3 by BASF, $La_{0.8}Ce_{0.2}CoO_3$ by Johnson Matthey, Co_2AlO_4/CeO_2 by Yara International, and FeZSM-5 by Uhde) [7]. Other catalytic systems have been recently evaluated under simulated conditions of adipic acid and nitric acid plants, such as yttrium-doped zirconias [8], $AB_{1-x}B'_xO_3$ perovskites with A = La or Ca, B = Mn or Fe, and B' = Cu or Ni [9], $ABAl_{11}O_{19}$ hexaaluminates with A = Ba or La and B = Fe, Mn, Co, or Ni) [10], α-alumina-supported iron oxide [11], and mayenite [12].

In contrast to chemical plants, catalytic technology for N_2O mitigation in fluidized-bed combustion has not been installed so far. The global N_2O emission from fossil-fuel combustion is estimated at 60–160 Mton CO_2-eq per year [13], without taking account the still uncertain emission from biomass and waste combustion. The overall figure likely exceeds the N_2O emission

* Corresponding author at: Laboratory for Heterogeneous Catalysis, Institute of Chemical Research of Catalonia (ICIQ), Avinguda Països Catalans 16, 43007, Tarragona, Spain. Tel.: +34 977 920 236; fax: +34 977 920 224.
E-mail address: jperez@iciq.es (J. Pérez-Ramírez).

0926-3373/$ – see front matter © 2009 Elsevier B.V. All rights reserved.
doi:10.1016/j.apcatb.2009.02.017

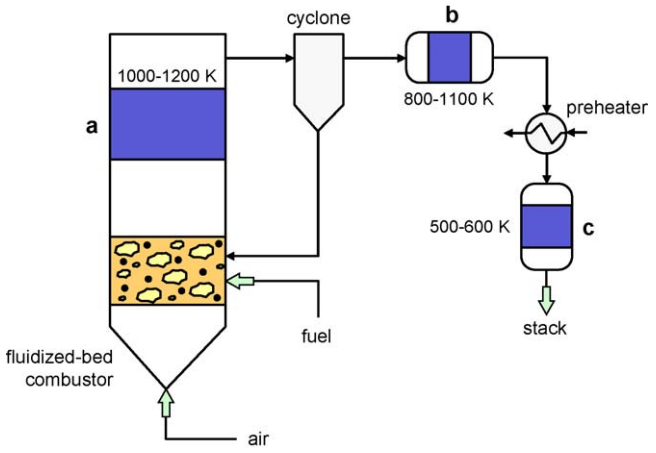

Fig. 1. Simplified flowsheet of a bubbling fluidized-bed combustor with possible locations for catalytic N_2O abatement. The position determines the main requirements for a suitable catalyst: high chemical stability and attrition resistance in (a) and low-temperature activity in (c). The location after the cyclone (b) is an intermediate case.

from nitric acid production (125 Mton CO_2-eq per year), which is currently the largest source in the chemical industry. Accordingly, the enforcement of environmental regulations for N_2O control in combustion processes can be foreseen in the short term. Additional incentive for producers comes from a recent directive that includes N_2O as a tradable gas under the EU Emission Trading Scheme for the period 2008–2012 [14].

In a bubbling fluidized-bed combustor, three locations for catalytic N_2O abatement can be potentially conceived (Fig. 1): (a) in the freeboard (1000–1200 K), (b) after the cyclone (800–1100 K), or (c) after the preheater (500–600 K). A major difficulty to develop robust de-N_2O catalysts in FBC off-gases stems from the complexity of the mixtures, containing N_2O, O_2, NO_x, CO, CO_2, SO_2, and H_2O. Several papers have addressed the de-N_2O activity of different catalysts in the presence of some of these gases [15–23], which often cause strong inhibition and deactivation. However, there is a clear lack of systematic studies including individual and combined effects of the components over representative catalysts. In particular, the sulfur tolerance is of primary importance for combustion applications and requires deeper analysis.

As starting point, it appears reasonable to evaluate whether existing de-N_2O catalysts for the aforementioned chemical plants are suitable for FBCs. It should be recalled that the extrapolation of catalytic technology from one source to another is often infertile, as de-N_2O catalysts are designed for particular conditions of feed composition, temperature, and pressure [7]. Herein, we have investigated Co_2AlO_4 spinel, $LaCoO_3$ perovskite, $BaFeAl_{11}O_{19}$ hexaaluminate, and FeZSM-5 zeolite for catalytic N_2O decomposition under realistic conditions of FBC off-gases. The catalytic performance was evaluated in model and simulated flue-gas mixtures and the effect of individual gaseous components for each catalyst was categorized. The three mixed oxide catalysts decompose N_2O beneath the Pt–Rh gauzes in ammonia burners of nitric acid plants [7,10], withstanding temperatures in the range 1073–1173 K and high concentrations of O_2, NO, and H_2O. Based on their remarkable chemical stability under harsh conditions, they can be regarded as potential candidates for de-N_2O in the freeboard of the combustor (Fig. 1). The iron zeolite, used for tail-gas N_2O abatement in nitric acid plants, is attractive because the rate of N_2O removal is accelerated by SO_2 [24]. However, tests were conducted in the absence of other relevant gaseous components such as NO, CO, and H_2O. Differently to previous works over iron-containing zeolites [17,22,23], the extra addition of hydrocarbons as reducing agents was explicitly avoided in order to maximize the cost effectiveness of the catalytic after-treatment. Based on our results, prospects for practical implementation are discussed.

2. Experimental

2.1. Catalyst preparation

The mixed oxides (Co_2AlO_4, $LaCoO_3$, and $BaFeAl_{11}O_{19}$) were prepared by coprecipitation of the corresponding precursors using the in-line dispersion precipitation (ILDP) method [25] followed by high-temperature calcination. An aqueous solution of the corresponding metal nitrates (spinel: 0.2 M Co and 0.1 M Al, perovskite: 0.1 M La and 0.1 M Co, and hexaaluminate: 0.1 M Ba, 0.1 M Fe, and 1.1 M Al) and an aqueous solution of 2 M Na_2CO_3 (spinel and perovskite precursors) or $(NH_4)_2CO_3$ (hexaaluminate precursor) were pumped into a 6 ml microreactor attached to a high-shear homogenizer rotating at 13,500 rpm. The pH of the slurry was measured and controlled by an in-line probe directly at the outlet of the precipitation chamber. Syntheses were carried out at constant pH 8 with an average residence time of 18 s. The slurries were aged at 333 K for 3 h, filtered, washed thoroughly, and dried at 353 K for 12 h. The resulting solids were calcined in static air at 1123 K (Co_2AlO_4), 1273 K ($LaCoO_3$), and 1473 K ($BaFeAl_{11}O_{19}$) for 10 h using a heating rate of 5 K min^{-1}. The preparation of steam-activated FeZSM-5 was detailed elsewhere [26]. Briefly, the isomorphously substituted iron zeolite was prepared by hydrothermal synthesis using TPA^+ as the template followed by calcination in static air (823 K, 10 h) and steam treatment (300 mbar H_2O and 30 ml STP N_2 min^{-1}, 873 K, 5 h).

2.2. Catalyst characterization

The chemical composition of the catalysts was determined by X-Ray Fluorescence (Philips PW 2400) and by Inductive Coupled Plasma-Optical Emission Spectroscopy (PerkinElmer Optima 3200RL (radial)). Powder diffraction patterns were measured in a Siemens D5000 diffractometer with Bragg-Brentano geometry and Ni-filtered Cu Kα radiation ($\lambda = 0.1541$ nm). Data were recorded in the range 5–70° 2θ with an angular step size of 0.05° and a counting time of 8 s per step. N_2 adsorption at 77 K was performed in a Quantachrome Autosorb 1-MP gas adsorption analyzer. Prior to analysis, the samples were degassed at 473 K for 6 h.

2.3. Activity tests

Activity tests were carried out in a MicroActivity Reference set-up (PID Eng&Tech) using a quartz microreactor (9 mm i.d.). The catalyst (0.1 g, sieve fraction 125–300 μm) was loaded between two layers of quartz wool and rested over a porous frit. The sample was pretreated in He at 673 K for 1 h and cooled down to the initial reaction temperature (473 K). Then, the feed mixture was introduced and the temperature was increased at intervals of 25–50 K up to 1123 K, using a heating rate of 5 K min^{-1} and keeping an isothermal period of 30 min at each set point. In this period of time, constant conversion levels were obtained and can be considered as the steady state. The experiments were carried out at ambient pressure using a space time ($W/F^\circ(N_2O)$) of 1245 g h mol^{-1}. Gas mixtures containing 0.3 mbar N_2O, 60 mbar O_2, 0.1 mbar NO, 0.14 mbar CO, 0.1 mbar SO_2, and 100 mbar H_2O in He were used. The N_2O conversion versus temperature curves for each feed composition were measured with a fresh catalyst sample. The stability of selected catalysts was studied by means of isothermal tests in the full gas mixture. Reactant and product gases were analyzed by a gas chromatograph (Agilent 6890N) equipped with HP-PLOT and DB-FFAP columns and TCD and FID detectors.

3. Results and discussion

3.1. Catalyst characterization

Prior to catalytic tests, the materials were subjected to basic characterization. The molar metal ratios in the mixed oxides determined by XRF were very close to the nominal values, indicating that the coprecipitation step was carried out effectively. As shown in Fig. 2, the X-ray diffraction patterns of the samples correspond to the desired pure phases: spinel (Co_2AlO_4, JCPDS 38-814), perovskite ($LaCoO_3$, JCPDS 25-1060), and hexaaluminate ($BaFeAl_{11}O_{19}$, JCPDS 26-135). Due to the high calcination temperature required for their crystallization, the bulk mixed oxides have a relatively low BET surface area, i.e. 20 $m^2\,g^{-1}$ in Co_2AlO_4, 4 $m^2\,g^{-1}$ in $LaCoO_3$, and 12 $m^2\,g^{-1}$ in $BaFeAl_{11}O_{19}$. The iron zeolite contains a molar Si/Al ratio of 31.3 and 0.67 wt.% Fe as determined by ICP. Extensive physico-chemical characterization of this specific catalyst was reported elsewhere [26–28] and will not be repeated here for the shake of conciseness. The material contains a distribution of extra-framework iron species in the form of isolated ions, oligonuclear species, and iron oxide nanoparticles of 1–2 nm.

3.2. Model versus simulated mixtures

First of all, the catalytic activity of the four catalysts was evaluated in model and simulated mixtures. Fig. 3a shows the N_2O conversion versus temperature in a feed containing only N_2O and O_2. The iron zeolite was the most active catalyst, displaying significant N_2O conversion above 700 K, followed by the spinel and the hexaaluminate. The perovskite resembles the spinel in the low-temperature region, shifting towards the hexaaluminate at higher temperatures. A quantitative comparison of the four catalysts can be given by the T_{50} (temperature at 50% N_2O conversion): 770 K for FeZSM-5, 860 K for Co_2AlO_4, and 900 K for $LaCoO_3$ and $BaFeAl_{11}O_{19}$.

Tests in the simulated FBC mixture, containing N_2O, O_2, NO, CO, SO_2, and H_2O rendered a completely different picture. The concentration of the components was selected attending to values in the literature for FBC flue-gases [13] and following advice from recognized experts in the field of coal combustion [29]. Comparison of the N_2O conversion curves in Fig. 3a and b makes it possible to conclude that the iron zeolite behaves similarly in the model and simulated mixtures (T_{50} = 770 K), while the de-N_2O activity of the mixed oxide catalysts is severely suppressed in the complex mixture with additional gases. For example, the T_{50} of Co_2AlO_4 shifts from 860 K in the model feed to 1050 K in the simulated feed. $BaFeAl_{11}O_{19}$ and $LaCoO_3$ suffered from a more pronounced inhibiting effect, particularly the perovskite. Accordingly, the activity differences are emphasized under realistic process conditions, enabling a proper discrimination of the catalysts. This statement is further supported by two particular examples. First of all, the light-off temperature in the model mixture is 100 K lower over the zeolite than over the spinel, and more than 350 K in the simulated mixture. Secondly, the simulated mixture evidences more pronounced activity differences between the three mixed oxide catalysts in comparison with the model mixture. In conclusion, these results highlight the absolute necessity of conducting experiments at conditions as close as possible to the real process in order to draw valid conclusions on their potential practical interest. It is sometimes felt that optimistic assessment of catalysts in the literature is made from tests in mixtures that contain only some of the relevant gases in the source under consideration.

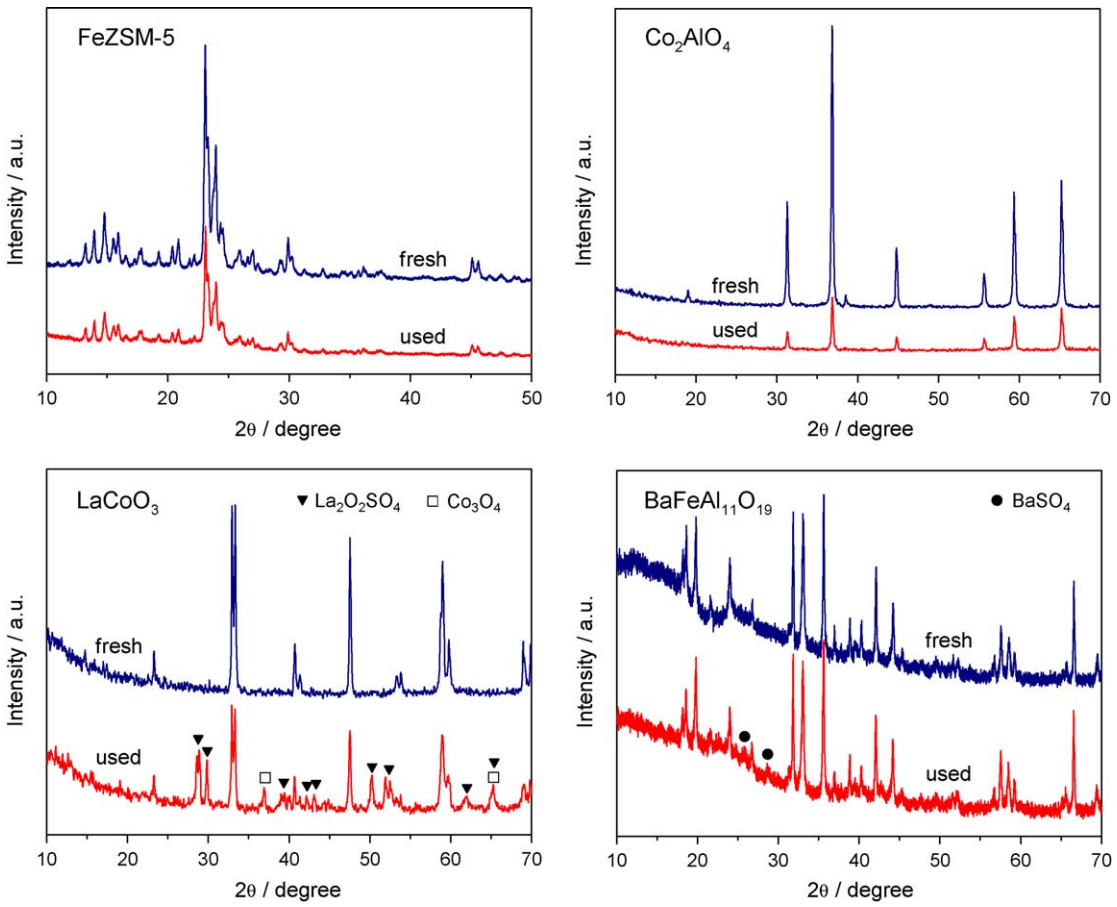

Fig. 2. X-ray diffraction patterns of the catalysts before and after catalytic tests in the simulated FBC mixture (see caption of Fig. 3).

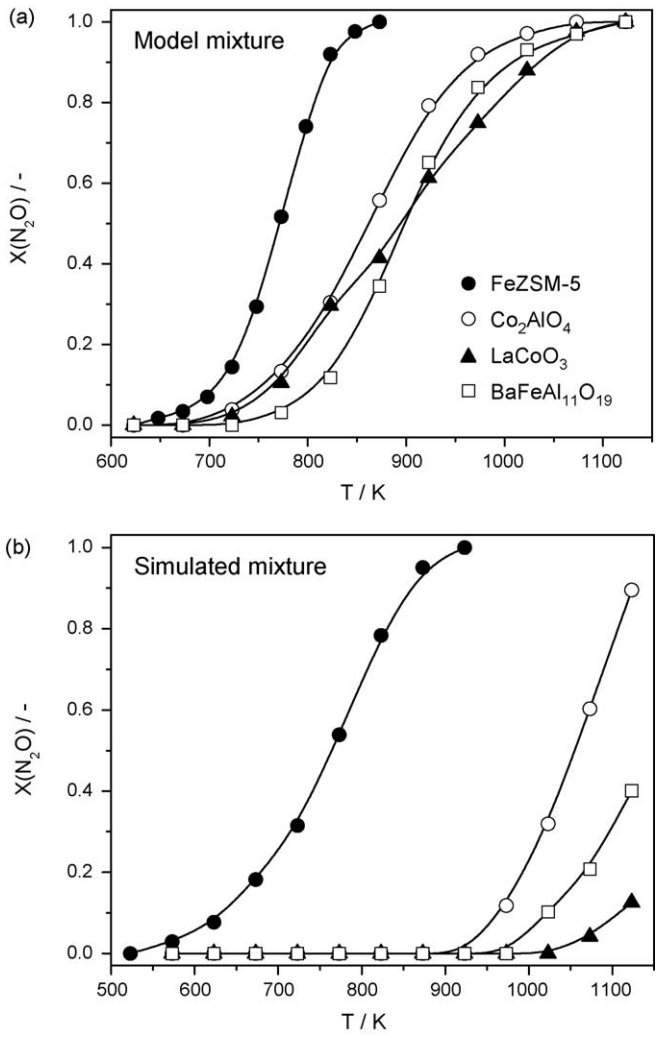

Fig. 3. N_2O conversion versus temperature over the catalysts in (a) model and (b) simulated mixtures. The model mixture contains 0.3 mbar N_2O and 60 mbar O_2 in He. The simulated mixture contains 0.3 mbar N_2O, 60 mbar O_2, 0.1 mbar NO, 0.14 mbar CO, 0.1 mbar SO_2, and 100 mbar H_2O in He. Other conditions: P = 1 bar and $W/F^{\circ}(N_2O)$ = 1245 g h mol^{-1}.

3.3. Effect of individual gases

The influence of each constituent of the gas mixture on the de-N_2O activity was investigated by adding one component to the $N_2O + O_2$ mixture over fresh catalyst. The resulting conversion profiles are depicted in Fig. 4. It can be seen that CO and NO affected to a minor extent the de-N_2O activity over the spinel, hexaaluminate, and perovskite catalysts. $LaCoO_3$ presented some inhibition by NO, most likely due to competitive adsorption with N_2O for active sites and/or to the formation of stable surface nitrate species. Water suppressed the catalytic activity to a much larger extent due to active site blockage, causing a shift of the N_2O conversion profiles by ca. 100–125 K to higher temperatures. The strongest inhibition was caused by sulfur dioxide, increasing the operation temperature by 200 K for the same degree of N_2O conversion. At low temperatures, the behavior of the mixed oxides is similar in the presence of SO_2, i.e. N_2O conversion is measurable above 923 K. However, in the high-temperature region, Co_2AlO_4 appears less affected than $LaCoO_3$ and $BaFeAl_{11}O_{19}$. The N_2O conversion in the full mixture was much lower than with the individual components, indicating that the combination of gases exerts a more detrimental effect on the catalytic activity. In fact, $LaCoO_3$ was completely inactive, since the conversion profile matched the conversion of the empty quartz reactor (gray line in Fig. 4). After the test in the simulated FBC gas mixture, the catalysts were re-tested in the model $N_2O + O_2$ mixture. All of them displayed a much lower N_2O conversion, confirming that the mixed oxides were severely deactivated under simulated conditions of FBC off-gases. Irreversible deactivation occurred when sulfur dioxide was present in the feed and particularly in combination with water.

The inhibition and deactivation of the mixed oxides by sulfur dioxide can a priori be attributed to sulfate formation. The drastic effect of SO_2 on the structural integrity of some of the mixed oxides due to extensive sulfation was confirmed by inspecting the X-ray diffraction patterns of the catalysts after the test in the simulated mixture. As seen in Fig. 2, the used catalysts were less crystalline than the fresh counterparts. More noticeably, the perovskite phase partially segregated into lanthanum oxysulfate ($La_2O_2SO_4$, JCPDS 41-678) and cobalt oxide (Co_3O_4, JCPDS 43-1003), while traces of baryte ($BaSO_4$, JCPDS 01-072-1378) were detected in the used hexaaluminate. Additional reflections belonging to bulk sulfate-containing or other phases were not detected in the pattern of Co_2AlO_4, suggesting that sulfation only occurs at a surface level.

The catalytic behavior of FeZSM-5 is radically different from those of the mixed oxides. The outcome is that the catalytic activity in the full mixture is somewhat higher than in the model mixture $<$773 K and slightly lower above this temperature (Fig. 4). The apparent activation energy of FeZSM-5 in $N_2O + O_2$ was estimated at 137 kJ mol^{-1}, being reduced to 86 kJ mol^{-1} in the simulated mixture. The unique tolerance of the steam-activated iron zeolite can be envisaged attending to works in the literature dealing with this specific catalytic system. Individually, the N_2O decomposition activity is not affected by O_2 [30], while NO [31], CO [32], and SO_2 [24] promote the catalytic N_2O removal with or without O_2 in the feed. As detailed in these publications, nitric oxide is a gaseous promoter and facilitates O_2 desorption via adsorbed NO_2 intermediates, while carbon monoxide and sulfur dioxide act as selective reducing agents scavenging adsorbed oxygen species deposited by N_2O. H_2O decreases the de-N_2O activity of steam-activated FeZSM-5, although its excellent hydrothermal stability in simulated tail-gases of nitric acid plants has been highlighted [30]. The combination of all these gases renders a catalyst yielding pretty comparable activity in the model and simulated mixtures. In our recent work over iron-containing zeolites with sulfur dioxide [24], tests were conducted in $N_2O + SO_2(+O_2)$, i.e. without other relevant gaseous components. Herein we show that the unique behavior of FeZSM-5 applies to simulated FBC mixtures. The X-ray diffraction pattern of the used iron zeolite was not altered (Fig. 3), although it experienced certain loss of crystallinity as generally noticed for the mixed oxides.

3.4. Stability

Stability tests were conducted over the spinel and zeolite catalysts. For this purpose, attending to the profiles in Fig. 3, the temperature was set at 773 K (FeZSM-5) and 973 K (Co_2AlO_4) in $N_2O + O_2$ and after 2 h, the simulated FBC mixture was introduced. In this manner, the short-term stability is studied at intermediate degrees of N_2O conversion. The N_2O conversion versus time is shown in Fig. 5. Co_2AlO_4 rapidly losses its activity, going from ca. 20% in the simulated mixture to practically no activity after 30 h on stream. Switching the feed back to the model feed at the same temperature led to a N_2O conversion of 45%, i.e. much lower than the ca. 90% of the fresh sample. This confirms the partial irreversible deactivation of the catalyst. In contrast, FeZSM-5 is stable during the 30-h period, keeping a fairly constant degree of N_2O conversion at ca. 65%.

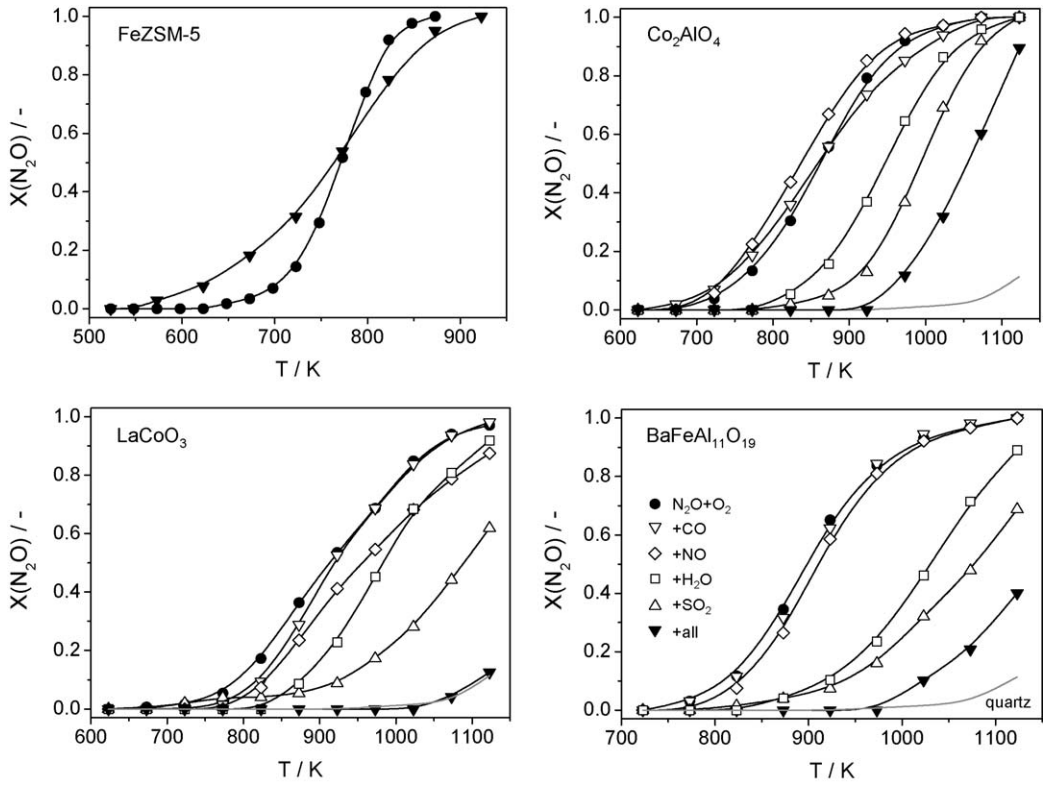

Fig. 4. N_2O conversion versus temperature over the catalysts in different mixtures, which are indicated in the legend of the hexaaluminate sample. The partial pressure of the components was 0.3 mbar N_2O, 60 mbar O_2, 0.1 mbar NO, 0.14 mbar CO, 0.1 mbar SO_2, and 100 mbar H_2O in He. Other conditions: P = 1 bar and $W/F^{\circ}(N_2O)$ = 1245 g h mol^{-1}. Gray line: N_2O conversion in a blank experiment with the empty quartz reactor.

Previous tests in the presence of water over this zeolite were conducted in mixtures with 1.5 vol.% H_2O [30], i.e. the characteristic content in the tail-gas of nitric acid plants. The water content in FBC off-gases is considerably higher (10 vol.% H_2O was used here). Due to this, zeolite dealumination can occur and might provoke structural damage, clustering of active iron species, and ultimately deactivation. Based on the stable N_2O conversion in Fig. 5, we believe that eventual dealumination of our zeolite in the catalytic tests was largely minimized. This is due to the particular preparation of the iron zeolite, specifically the treatment in a stream of inert containing 30 vol.% H_2O at 873 K for 5 h. This activation step, which is primarily intended for dislodgement of isomorphously substituted iron towards active extra-framework positions, also causes partial dealumination [26–28]. In our opinion, the treatment effectively stabilizes the zeolite for subsequent use in wet waste streams since both temperature and steam content are more severe in the activation step than under optimal operating FBC conditions. We inspected the used zeolite after the isothermal stability test by transmission electron microscopy, observing that the size of the visible iron oxide nanoparticles was not altered, e.g. due to clustering and sintering, with respect to the fresh zeolite (not shown). Additional characterization of intracrystalline iron species such as isolated ions and oligonuclear clusters in the zeolite pores is beyond the scope of this paper and would be needed to confirm the no alternation of the iron speciation.

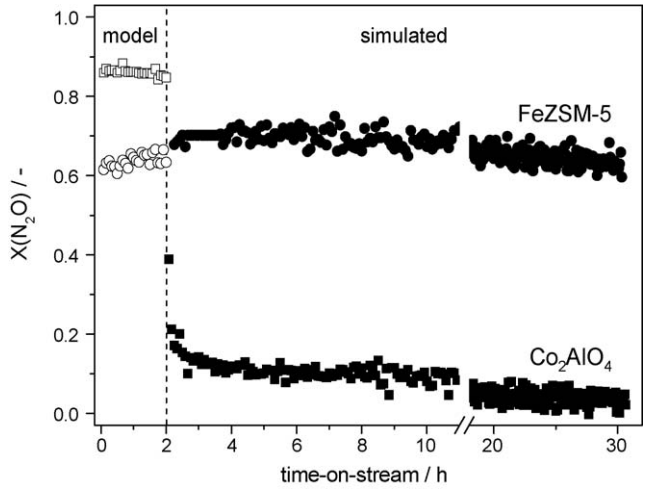

Fig. 5. N_2O conversion versus time-on-stream over FeZSM-5 (circles) at 773 K and Co_2AlO_4 (squares) at 973 K in model and simulated mixtures. Conditions as in caption of Fig. 3.

3.5. Opportunities for implementation in FBC

The implementation of N_2O abatement technology in flue-gases of fluidized-bed combustors should likely occur within the next few years due to (i) the significant emission, even exceeding that of chemical production processes, (ii) the enforcement of environmental regulations by governments, and (iii) the recent inclusion of N_2O as a tradable greenhouse gas under the EU Emission Trading Scheme. The extrapolation of catalytic systems operative in chemical plants to FBCs is not straightforward due to the distinct conditions. The presence of SO_2 combined with high concentrations of H_2O characteristic of combustion processes are critical aspects to develop stable catalysts. The spinel, perovskite, and hexaaluminate catalysts evaluated in this study proved highly stable for process-gas N_2O decomposition in ammonia burners of nitric acid plants, i.e. withstanding high temperatures (1073–1173 K) and the presence of high concentrations of O_2, NO, and H_2O

[7,10]. However, the mixed oxides are very sensitive to sulfur and the presence of water, experiencing rapid deactivation. The chance of implementing such system in FBCs, e.g. in the freeboard of a bubbling fluidized-bed, is remote in view of their limited chemical stability whenever sulfur dioxide is present. The same outcome in this or other location of the process is expected over other active N_2O decomposition catalysts such as Rh/Al_2O_3 [15], Rh/ZrO_2 [20], Ru/Al_2O_3 [33], calcined Co–Al hydrotalcites with Rh or Pd [34], Co–ZSM-5 [35], and Cu–ZSM-5 [35,36], since they are also strongly inhibited and or deactivated by SO_2. The sulfur tolerance is of primary importance to develop robust catalysts in environmental applications associated with combustion sources, not only for N_2O abatement but also for NO_x storage and reduction [37–39] and hydrocarbon oxidation [40,41].

Promising results arise from the application of steam-activated FeZSM-5 zeolite. This system is unique since its de-N_2O activity is promoted by components coined as inhibitors and poisons for most catalysts (mainly NO and SO_2). Stable performance has been obtained during 30 h on stream at 773 K. This temperature is too high for eventual installation of the catalyst after the preheater, where the temperature does not exceed 600 K (position c in Fig. 1). Addition of hydrocarbons (e.g. propane) could lower the operating temperature of the iron zeolite [22,23]. However, reaching a complete degree of N_2O conversion remains challenging at such low temperature. In addition, the operating cost of the 'selective catalytic reduction' option is prohibitive compared to the 'direct decomposition' option [7]. The location of the iron zeolite catalyst after the cyclone (Fig. 1, position b) appears suitable attending to the available temperature (800–1100 K). As discussed above, the synthesis route of FeZSM-5 is considered to be a decisive factor for its stable behavior. The steam treatment of our catalyst under conditions (temperature, steam content) exceeding its operation in FBCs is advisable to stabilize the zeolite framework and distribution of iron species in the material.

4. Conclusions

The extrapolation of commercial catalysts for N_2O abatement in chemical plants to stationary combustion sources such as fluidized-bed combustions requires careful consideration. In spite of their remarkable performance for process-gas N_2O abatement in nitric acid plants, mixed oxide catalysts such as Co_2AlO_4, $LaCoO_3$, and $BaFeAl_{11}O_{19}$, lack chemical stability and experience severe deactivation under FBC conditions, mainly due to the presence of SO_2 and H_2O. Steam-activated FeZSM-5 zeolite displays remarkable activity and stability and is a serious candidate for practical implementation in stationary combustion facilities.

Acknowledgements

This research was funded by the Spanish MEC (project CTQ2006-01562/PPQ and Consolider-Ingenio 2010 Grant CSD2006-0003) and the ICIQ Foundation.

References

[1] http://www.worldcoal.org, January 3, 2009.
[2] S.N. Oka, Fluidized Bed Combustion, Marcel Dekker, New York, 2004.
[3] M.A. Wójtowicz, J.R. Pels, J.A. Moulijn, Fuel Process. Technol. 34 (1993) 1.
[4] L. Armesto, H. Boerritger, A. Bahillo, J. Otero, Fuel 82 (2003) 1845.
[5] M.J. Fernandez Gutierrez, D. Baxter, C. Hunter, K. Svoboda, Waste Manage. Res. 23 (2005) 133.
[6] A. Shimizu, K. Tanaka, M. Fujimori, Chemosphere 2 (2000) 425.
[7] J. Pérez-Ramírez, F. Kapteijn, K. Schöffel, J.A. Moulijn, Appl. Catal. B 44 (2003) 117.
[8] P. Granger, P. Esteves, S. Kieger, L. Navascues, G. Leclercq, Appl. Catal. B 62 (2006) 236.
[9] S. Alini, F. Basile, S. Blasioli, C. Rinaldi, A. Vaccari, Appl. Catal. B 70 (2007) 323.
[10] J. Pérez-Ramírez, M. Santiago, Chem. Commun. (2007) 619.
[11] G. Giecko, T. Borowiecki, W. Gac, J. Kruk, Catal. Today 137 (2008) 403.
[12] M. Ruszak, M. Inger, S. Witkowski, M. Wilk, A. Kotarba, Z. Sokja, Catal. Lett. 126 (2008) 72.
[13] F. Kapteijn, J. Rodríguez-Mirasol, J.A. Moulijn, Appl. Catal. B 9 (1996) 25.
[14] Reference COD/2008/0013, amendment of Directive 2003/87/EC, more details available at http://ec.europa.eu/environment/climat/emission, January 3, 2009.
[15] T. Dann, K.H. Schulz, M. Mann, M. Collings, Appl. Catal. B 6 (1995) 1.
[16] J. Rodríguez-Mirasol, E. Ito, C.M. van den Bleek, L. Monceaux, P. Courtine, F. Kapteijn, J.A. Moulijn, in: J.A. Pajares, J.M.D. Tascón (Eds.), Coal Science, Elsevier Science, Amsterdam, 1995, pp. 1911–1914.
[17] G. Centi, F. Vazzana, Catal. Today 53 (1999) 683.
[18] E. Sasaoka, N. Sada, K. Hara, Md. Azhar Uddin, Y. Sakata, Ind. Eng. Chem. Res. 38 (1999) 1335.
[19] T. Shimizu, M. Hasegawa, M. Inagaki, Energy Fuels 14 (2000) 104.
[20] G. Centi, S. Perathoner, F. Vazzana, M. Marella, M. Tomaselli, M. Mantegazza, Adv. Environ. Res. 4 (2000) 325.
[21] J. Pérez-Ramírez, F. Kapteijn, G. Mul, J.A. Moulijn, Appl. Catal. B 35 (2002) 227.
[22] E. Ruiz-Martínez, J.M. Sánchez-Hervás, J. Otero-Ruiz, Appl. Catal. B 50 (2004) 195.
[23] E. Ruiz-Martínez, J.M. Sánchez-Hervás, J. Otero-Ruiz, Appl. Catal. B 61 (2005) 306.
[24] J. Pérez-Ramírez, M.A.G. Hevia, S. Abelló, Chem. Commun. (2008) 5351.
[25] M. Santiago, M.S. Yalfani, J. Pérez-Ramírez, J. Mater. Chem. 16 (2006) 2886.
[26] J. Pérez-Ramírez, G. Mul, F. Kapteijn, J.A. Moulijn, A.R. Overweg, A. Doménech, A. Ribera, I.W.C.E. Arends, J. Catal. 207 (2002) 113.
[27] J. Pérez-Ramírez, F. Kapteijn, J.C. Groen, A. Doménech, G. Mul, J.A. Moulijn, J. Catal. 214 (2003) 33.
[28] J. Pérez-Ramírez, J. Catal. 227 (2004) 512.
[29] A. Bahillo, J.M. Sánchez-Hervás, CIEMAT Madrid, personal communication, 2008.
[30] J. Pérez-Ramírez, F. Kapteijn, G. Mul, J.A. Moulijn, Chem. Commun. (2001) 693.
[31] J. Pérez-Ramírez, F. Kapteijn, G. Mul, J.A. Moulijn, J. Catal. 208 (2002) 211.
[32] J. Pérez-Ramírez, M. Santosh Kumar, A. Brückner, J. Catal. 223 (2004) 13.
[33] G.E. Marnellos, E.A. Efthimiadis, I.A. Vasalos, Appl. Catal. B 46 (2003) 523.
[34] J. Pérez-Ramírez, F. Kapteijn, J.A. Moulijn, Catal. Lett. 60 (1999) 133.
[35] F. Kapteijn, G. Mul, G. Marbán, J. Rodríguez-Mirasol, J.A. Moulijn, Stud. Surf. Sci. Catal. 101 (1996) 641.
[36] A.J.S. Mascarenhas, H.M.C. Andrade, React. Kinet. Catal. Lett. 64 (1998) 215.
[37] S. Hodjati, C. Petit, V. Pitchon, A. Kiennemann, Appl. Catal. B 30 (2001) 247.
[38] P.T. Fanson, M.R. Horton, N.W. Delgass, J. Lauterbach, Appl. Catal. B 46 (2003) 393.
[39] K.-I. Shimizu, T. Higashimata, M. Tsuzuki, A. Satsuma, J. Catal. 239 (2006) 117.
[40] J. Beckers, L.M. van der Zande, G. Rothenberg, ChemPhysChem 7 (2006) 747.
[41] A.M. Venezia, R. Murania, G. Pantaleo, G. Deganello, J. Catal. 251 (2007) 94.